

LATTICE-GAS MODELS: A NEW ROUTE FOR HYDRODYNAMICS

P.C. Philippi & L.O.E. dos Santos

Laboratório de Meios Porosos e Propriedades Termofísicas (LMPT)

Departamento de Engenharia Mecânica

Universidade Federal de Santa Catarina

CX P 476 88040-900 Florianópolis SC

philippi@lmpt.ufsc.br, emerich@lmpt.ufsc.br

1. INTRODUCTION

Considering the macroscopic description of fluid flow, lattice gas models are to be considered as *lower-level* models based on the statistical behavior of a large set of particles moving along the discrete directions of a regular lattice and colliding in lattice vertices.

In fact, there are important physical phenomena related to fluid flow that are difficult to, or cannot, be described by considering the only information given by the macroscopic equations, at the macroscopic level. In these cases *downscaling* to a lower scale is, often, necessary for the correct understanding and mathematical description of the particular physical phenomena of interest.

Some of these phenomena, related to interfacial dynamics, are presented bellow

When two droplets of a fluid r are put very close, Figure 1.1, long-range fields arising from each one of the droplets attract molecules belonging to the second droplet, giving rise to *coalescence*. Coalescence is a very difficult interfacial phenomenon, which can, only, be fully described, in the molecular scale, related to interaction length of long-range forces.

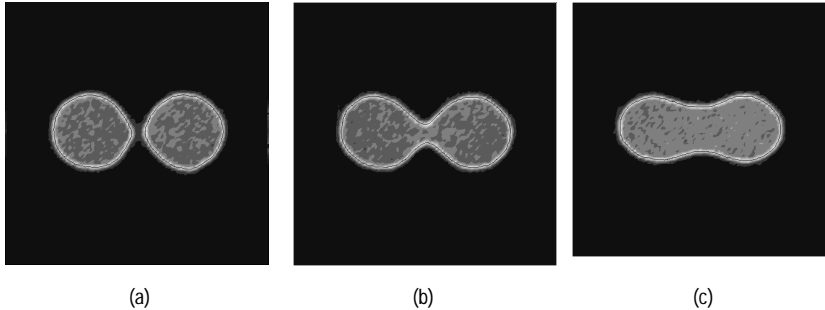


Figure 1.1. Coalescence between two droplets.

Although very interesting from a physical point of view, droplet formation from a dropper is a very difficult problem, when we consider classical discrete methods of fluid mechanics. Droplet formation of mineral oil in water is pictured in Figure 1.2, showing a sequence of photographs taken at 10 frames/s.

From a macroscopic point of view droplet's shape time evolution is linked to the competition it is subjected among gravity action, viscosity of the droplet fluid and interfacial tension. In this way, interfacial forces hold the droplet until break-off, as droplet

weight increases. Break-off starts with the development of a throat, which becomes thinner in time and from where droplet fluid is pulled downward and redistributed horizontally by viscous forces, giving an almost ellipsoidal shape to the falling droplet, with a major axis oriented along horizontal direction.

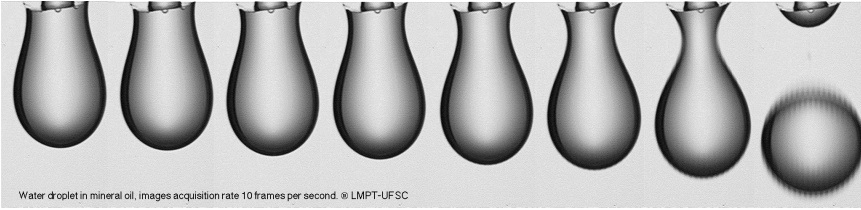


Figure 1.2 Droplet formation.

Lattice gas models were, firstly, developed for single-phase flows based, mainly, on *cellular automata* and on *kinetic theory*. Two classes of models have been developed: Boolean and lattice Boltzmann models.

Although kinetic theory dates from Bernoulli (1738), who tried to explain *elasticity* of gases considering them as a set of particles in random motion, its main development occurred in the second half of XIX century by Maxwell and Boltzmann. This was achieved introducing *probability theory* in the study of N-body problem in classical Lagrangian mechanics.

In fact, no *general* solution exists for the N-body problem when N is larger than 2.

Considering a gas as a set of a *very large* number N of material points, with translational degrees of freedom, it is possible to use probability laws, considering

$$f(\mathbf{r}, \mathbf{c}, t),$$

as a probability density function for the number of particles with velocities between \mathbf{c} and $\mathbf{c} + d\mathbf{c}$ found, at time t , inside an elementary volume $d\mathbf{r}$ of the physical space.

Considered as a continuous function, the velocity distribution function $f(\mathbf{r}, \mathbf{c}, t)$ is modified in the absence of external forces by the streaming of particles and by collisions in \mathbf{r}, \mathbf{c} space. Its evolution is given by Boltzmann's equation:

$$\partial_t f + \mathbf{c}_\alpha \partial_\alpha f = (\partial_t f)_{\text{coll}}, \quad (1.1)$$

where ∂_t is a time derivative and ∂_α means a spatial derivative.

Boltzmann's equation has an H-theorem and an equilibrium solution, explaining irreversibility of macroscopic behavior as due to inter-particle collisions. In this way, collisions are considered to be the main mechanism responsible for dissipation phenomena in fluids.

In the early XX century, Chapman and Enskog, simultaneously, formally retrieved hydrodynamic transport equations from Boltzmann's equation, by considering the first statistical moments of the velocities distribution function (Chapman and Cowling, 1970):

$$\partial_t \langle \rho \rangle + \partial_\beta \langle \rho v_\beta \rangle = 0, \quad (1.2)$$

$$\partial_t \langle \rho v_\alpha \rangle + \partial_\beta \langle \rho v_\alpha v_\beta \rangle = -\partial_\alpha \langle \rho \rangle + \partial_\beta \langle \mu [\partial_\beta \langle v_\alpha \rangle + \partial_\alpha \langle v_\beta \rangle] \rangle + \partial_\alpha \langle \kappa [\partial_\beta \langle v_\beta \rangle] \rangle, \quad (1.3)$$

where \mathbf{v} designates fluid velocity.

In the above equations: i) pressure p is directly related to mass density ρ by ideal gas law, ii) first, μ , and second, κ , viscosity coefficients are given in terms of the collision term in the Boltzmann's equation and related to ideal gas behavior.

These two above remarks are very important in the context of lattice gas development. In fact, it means that: a) a set of particles follow ideal gas law, when *long-range* interaction are not considered; b) hydrodynamic equations are *insensible* to the details of collision processes, which appear related, only, to the transport coefficients themselves μ and κ .

The last observation was the basis for the development of LGA models.

Boolean lattice gas automata models (LGA) are microscopic models based on particles, which dynamics try to mimic the main overall dynamics of a large set of molecules, preserving mass, momentum and, more recently, energy.

In Boolean models, a Boolean variable $n_i(X,T)$ is attributed to direction i of each site X of a discrete lattice, at time step T , indicating the presence ($n_i=1$) or absence ($n_i=0$) of a fluid particle, following an exclusion principle. For each time step, the dynamic evolution of the model is given in two steps. In the first step, designated as *collision step*, the state of site X is changed following collision rules conceived so as to preserve total mass and momentum of the site. In the second step, called *propagation step*, particles are propagated to the neighbor sites, in accordance with their direction at site X after collision step. The use of such models to study and simulate fluid dynamics was firstly introduced by Hardy, de Pazzis and Pomeau (1973, 1976), but it was only after 1986 that these models grew in increased importance due to the work of Frisch *et al.* (1986, 1987) These authors formally demonstrated that the dynamics of such models under certain conditions was described by the Navier-Stokes equations for incompressible flows, and could be used to simulate such flows. In fact, based on a square two-dimensional lattice, HPP model of Hardy *et al.* (1973): i) does not have isotropic fourth-order tensors, such as viscosity and ii) preserves spurious quantities, giving a non-physical behavior to the model. See also Wolfram (1983,1984,1986).

The main contribution of Frish *et al.* (1986), was to demonstrate that hexagonal lattices have the necessary number of degrees of freedom to give isotropic fourth-order viscosity tensor and the elimination of spurious invariants. In three-dimensions, isotropy has been investigated by d'Humières *et al.* (1986), who introduced the three-dimensional projection of a four-dimensional lattice, the face-centered hypercubic lattice (FCHC) as the simplest lattice giving isotropy of fourth-order tensors. FCHC lattices have 24 degrees of freedom.

Although very suitable from a computational point of view, regarding parallelism and numerical stability, the use of Boolean variables has very serious limitations that may be summarized by considering: i) non-physical terms in macroscopic equations due to exclusion principle, ii) high noise/signal level, produced by excessively drastic transitions and requiring spatial averages and iii) high transport coefficients.

For this reason, LGA models have been, gradually, replaced by Boltzmann, mesoscale models, in practical applications, although some work is, very recently, being undertaken, for reducing, or eliminating, these drawbacks.

At mesoscale, lattice Boltzmann equation (LBE) resulted from the statistical averaging $N_i = \langle n_i \rangle$ of a large set of realizations of Boolean evolution equation, considering molecular-chaos hypothesis (McNamara and Zanetti, 1988). Fluctuations were drastically

reduced in simulating $N_i(\mathbf{X}, T)$, but the remaining drawbacks of Boolean models were preserved. Higuera and Jimenez (1989) proposed the use of a linearized collision term, further simplified by Qian et al. (1992) to give a single relaxation time model. In its present form, LBE is to be considered as a mesoscale relaxation equation, which main *collision term* does not follow Boolean transitions, but is written following some main fundamental principles, such as mass and momentum conservation and considering lattice symmetries.

In addition of enabling the description of physical process that require downscaling, lattice Boltzmann models present some computational features that can be forwarded to persuade CFD practitioner to adopt these models in simulating fluid flow: simplicity of the algorithm, easy of dealing with complicated geometric boundaries and high level of parallelism in the implementation.

This lecture is organized in the following manner. In Section 2, Boolean lattice gas models are discussed. Section 3 is devoted to Boltzmann mesoscale models, based on LBE relaxation equation. Section 4 gives a brief introduction to multibits and integers models. Section 5 present a Boolean model based on field mediators for studying the flow of miscible and immiscible fluids. Boltzmann's counterparts are presented in Sections 6 and 7.

2. BOOLEAN MODELS FOR MONOPHASIC FLOWS

2.1 Microscopic Dynamics

Consider a regular lattice, Figure 2.1, where each site \mathbf{X} has b_m neighbors. A Boolean variable $n_i(\mathbf{X}, T)$ is assigned to site \mathbf{X} to indicate the presence ($n_i=1$) or absence ($n_i=0$) of a particle in direction i at time T . Vector \mathbf{c}_i indicates the unitary velocity vector pointing in direction i . A finite, at most b_r , number of, undistinguishable, rest particles is allowed to populate site \mathbf{X} . Let $b = b_m + b_r$. Let S be the set of all possible states of a given lattice site.

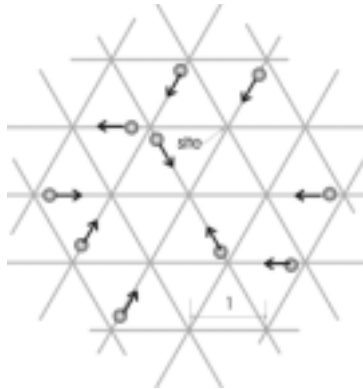


Figure 2.1. A two-dimensional hexagonal lattice.

A given state s of S can be represented by the array:

$$s = (s_{01}, \dots, s_{0b_r}, s_1, \dots, s_{b_m}), \quad (2.1)$$

where the first b_r bits indicate rest particles and the following b_m bits indicate moving particles, distributed along the b_m lattice directions.

Microscopic evolution is described by the following equation:

$$n_i(\mathbf{X}+\mathbf{c}_i, T+1)=n_i(\mathbf{X}, T) + \omega_i(n_{o1}, \dots, n_{obr}, n_1, \dots, n_{bm}), \quad (2.2)$$

where $\omega_i: (n_{o1}, \dots, n_{obr}, n_1, \dots, n_{bm}) \rightarrow \{-1, 0, 1\}$ represents the collision operator which can take the values -1 , 1 or 0 , depending on the state $(n_{o1}, \dots, n_{obr}, n_1, \dots, n_{bm})$ of site \mathbf{X} , before the collision.

Considering $\xi(\mathbf{X}, T)$ to be a random number attributed to site \mathbf{X} at time T and $\alpha_{\xi(\mathbf{X}, T)}(s, s')$ to be the transition matrix changing state s to one of all possible post-collision states s' , in accordance with $\xi(\mathbf{X}, T)$, collision term can be written as

$$\omega_i(n_{o1}, \dots, n_{obr}, n_1, \dots, n_{bm}) = \sum_s \left[\sum_{s'} \alpha_{\xi(\mathbf{X}, T)}(s, s')(s'_i - s_i) \prod_{j=1}^b \delta(n_{ji}, s_j) \right] \quad (2.3)$$

2.2 Ensemble averages. Macroscopic behavior of LGA model.

Lattice-gas models have three description levels. In the more detailed level, $n_i(\mathbf{X}, T)$ are described for every \mathbf{X} and T . In general, this is too refined in the description of macroscopic phenomena. A less detailed description is given by furnishing the expected values $N_i = \langle n_i(\mathbf{X}, T) \rangle$, obtained as *ensemble* averages over a large number of realizations. In the third level, only the first moments of N_i are furnished for each \mathbf{X} and T . In fact, in the continuum limit, when Knudsen number is very small, it can be shown that the first moments of N_i are related between themselves through a closed system of equations, i.e., the hydrodynamic equations.

Classically, in the framework of *hydrodynamics*, we try to solve this closed system of equations and obtain numerical values for pressure, density and velocity fields. In LGA conception, expected values $N_i(\mathbf{X}, T)$ result from several realizations of a given Boolean model. Macroscopic equations are, then, obtained from the first moments of N_i . It can be shown that, under certain restrictions, these moments satisfy classical hydrodynamic equations (Frish *et al.*, 1986).

Distribution $N_i(\mathbf{X}, T)$ is defined as the expected value of $n_i(\mathbf{X}, T)$, over an *ensemble* of realizations, run using randomly chosen initial conditions and satisfies.

$$N_i(\mathbf{X}+\mathbf{c}_i, T+1)=N_i(\mathbf{X}, T) + \Omega_i(N_o, N_1, \dots, N_{bm}), \quad (2.4)$$

which is Boltzmann equation for the lattice, in discrete form. Since rest particles are undistinguishable, $N_o(\mathbf{X}, T)$ means the probability of finding rest particles on site \mathbf{X} at time T , in several realizations. Taking molecular chaos hypothesis into account, the collision term can be written as:

$$\Omega_i(N_o, N_1, \dots, N_{bm}) =$$

$$\langle \omega_i(n_{o1}, \dots, n_{obr}, n_1, \dots, n_{bm}) \rangle = \sum_s \left[\sum_{s'} A(s, s') (s'_i - s_i) \prod_{j=1}^b N_j^{s_j} (1 - N_j)^{1-s_j} \right]. \quad (2.5)$$

In the above equation,

$$A(s, s') = \langle \alpha(s, s') \rangle. \quad (2.6)$$

Using the semi-detailed balance condition,

$$\sum_s A(s, s') = 1, \quad \forall s', \quad (2.7)$$

it can be shown that Eq. (2.4) has an H-Theorem and an equilibrium solution ,

$$N_i^0 = \frac{1}{1 + \exp(\alpha + \mathbf{q} \cdot \mathbf{c}_i)}, \quad (2.8)$$

which is a Fermi-Dirac distribution, as a consequence of *exclusion principle*.

Due to the discrete nature of the model, a linear low velocity approximation is used, written in terms of the density

$$\rho = \sum_{i=1}^{b_m} N_i + N_o b_r, \quad (2.9)$$

and the mean velocity

$$\mathbf{u} = \frac{1}{\rho} \sum_{i=1}^{b_m} N_i \mathbf{c}_i, \quad (2.10)$$

which can be used for finding constants α and \mathbf{q} .

This equilibrium solution can be written as

$$N_i^0 = f \left[1 + \frac{D b}{c^2 b_m} c_{i\alpha} u_\alpha + \frac{D^2 b^2}{2c^4 b_m^2} \left(\frac{1-2f}{1-f} \right) \left(c_{i\alpha} c_{i\beta} - \frac{c^2}{D} (1-b_r) \delta_{\alpha\beta} \right) u_\alpha u_\beta \right] + O(u^3), \quad (2.11)$$

for moving particles whereas for rest particles,

$$N_o^0 = f \left[1 - \frac{D}{2c^2} \frac{b}{b_m} \left(\frac{1-2f}{1-f} \right) u^2 \right] + O(u^4). \quad (2.12)$$

In the above equations D is the Euclidean dimension of the lattice and $f = \rho/b$.

2.3 Lattice Gas Hydrodynamic Equations

The use of Chapman-Enskog method on the N_i evolution equation, Eq.(2.4), leads to lattice gas hydrodynamic equations, in the limit of low Knudsen number, Kn and low Mach number, M :

$$\partial_t(\rho) + \partial_\beta(\rho u_\beta) = 0 \quad (2.13)$$

$$\partial_t(\rho u_\alpha) + \partial_\beta \left[g(\rho) \rho u_\alpha u_\beta \right] = -\partial_\alpha(p(\rho, u^2)) + \nu \partial_\beta \left[\partial_\beta(\rho u_\alpha) + \partial_\alpha(\rho u_\beta) \right] + \eta \partial_\alpha \left[\partial_\beta(\rho u_\beta) \right] \quad (2.14)$$

where

$$g(\rho) = \frac{bD}{b_m(D+2)} \left(\frac{1-2f}{1-f} \right) \quad (2.15)$$

$$p(\rho, u^2) = c_s^2 \rho - M^2 \rho g(\rho) \left(1 + \frac{D}{2} - \frac{bD}{2b_m} \right) \quad (2.16)$$

and $c_s^2 = \frac{b_m c^2}{bD}$ is the square of LGA sound speed. The first and the second viscosity coefficients, respectively ν and η , are related to the eigenvalues of collision operator Ω . Equations (2.13) and (2.14) differ from Navier-Stokes hydrodynamic equations: i) by the inclusion of a $g(\rho)$ dependence in the inertial term, breaking Galilean invariance, ii) by a $O(M^2)$ additional term in the pressure equation, Eq. (2.16), considering U as a characteristic macroscopic speed, in lattice units and taking M as the Mach number, $M = U/c_s$, and iii) by the inclusion of density ρ *inside* the spatial derivatives in the viscous terms. In low Mach numbers limit (Rothman and Zaleski, 1997), the incompressibility condition

$$\nabla \cdot \mathbf{u} = 0 \quad (2.17)$$

is recovered and the following momentum equations are found, in this limit :

$$\rho \partial_t(u_\alpha) + \rho g(\rho) u_\beta \partial_\alpha u_\beta = \partial_\alpha(p) + \rho \nu \partial_\beta \partial_\beta u_\alpha, \quad (2.18)$$

which are the correct Navier-Stokes equations, for incompressible flows, excepting by the inclusion of a $g(\rho)$ factor in the inertial term. Considering Eq. (2.15), it can be seen that $g(\rho) \rightarrow 1$ when the following two conditions are, simultaneously, satisfied.

a) Factor

$$(1-2f)/(1-f) \rightarrow 1, \quad (2.19)$$

related to the fact that lattice effects due to *exclusion principle* are reduced, when reducing lattice density.

b) Factor

$$\frac{bD}{b_m(D+2)} \rightarrow 1 \quad (2.20)$$

meaning that lattice effects due to the use of a *finite number of directions* are reduced, when increasing the number of lattice degrees of freedom, increasing $b_l = b - b_m$ for rest particles,

for compensating factor $D/(D+2) < 1$ and/or working with three-dimensional lattice projections of higher D hyper-spaces.

The first alternative is limited by *noise increase* in the simulations, requiring the use of larger spatial averages. The second one is limited to computer resident-memory capacity, as memory requirements increase with $(b_r + 1) 2^{bn}$.

Lattice effects can be, also avoided by rescaling variables \mathbf{u} and p (Rothman and Zaleski, 1997), which is a, presently, frequently used simulation *strategy*.

2.4 Sample application: prediction of intrinsic permeability of porous rocks: Santos (2000), Santos et al. (a-b) (2000), Santos et al.(a) (2002).

At author's knowledge, lattice-gas hydrodynamic models for flow through two and three-dimensional artificially constructed porous microstructures were described by Chen *et al.* (1991.b). Kohring (1991a-b), Kohring (1992), McCarthy (1994), and Gao and Sharma (1994) introduced lattice-gas models for studying the flow through channels, random array of solid obstacles and/or regular arrays of cylinders. Ginsbourg and Adler (1994), Genabeek and Rothman (1999) and Bernabe and Olson (2000) produced detailed results related to boundary location and to the influence of surface topography on the flow rate, for flow inside channels with rough surfaces.

Lattice-Boltzmann method was applied for reconstructed three-dimensional porous microstructure by Ferreol and Rothman (1995) and by Singh and Mohanty (2000).

Boolean models are *lower level* models with respect to lattice Boltzmann. In present application, the use of Boolean models is proposed for the prediction of intrinsic permeability. In contrast with lattice-Boltzmann method, which is free from intrinsic noise, Boolean models present, nevertheless, very attractive advantages from a computational point of view, as simulations are performed with Boolean variables needing less resident memory capability and reducing running time. Taking into account that intrinsic permeability is a *global property*, *spatial averages* can be performed considering the whole pore space. In addition, ergodic hypothesis enables the use of unrestricted *time averages*. In this presentation it is shown that, as a consequence of spatial and time averages, reduction of intrinsic fluctuations of Boolean models, leads to the prediction of very stable values of intrinsic permeability, when simulation is performed considering a sufficiently great number of time steps.

2.4.1 Simulation scheme

Evolution equation, Eq. (2.2), is the basic algorithm used for simulating flow. At time $t=0$, lattice particles are randomly distributed on the lattice sites. For each pre-collision configuration s , post-collision configuration s' is randomly chosen between those states s' with the same mass and momentum. This is performed by using a transition table located in computer resident memory and constructed, previously to simulation, following the particular LGA model used. Model is based on a FCHC lattice with $b=24$ (d'Humières *et al.*, 1986). In propagation step, each particle at direction i is propagated to the neighbor site $\mathbf{X} + \mathbf{c}_i$.

At solid boundaries, particles that reached boundary sites are bounced back, at the next time step. This is the *bounce-back* condition that is frequently used, avoiding flow slipping at the boundary, and assuring adherence condition, $\mathbf{u}=\mathbf{0}$.

In simulating incompressible flows, considering the state equation relating pressure to density, pressure gradients can, only, be promoted, associated to density gradients, which must, in turn, remain small. This problem is eschewed in conventional simulation by using Navier-Stokes *low Mach number, M , approximation*. Nevertheless, in LGA simulation, flow is the result of *billiard balls* collisions and incompressibility can only be assured by working with small $|\mathbf{u}|$ meaning small $M=u/c_s$. It can be show that $c_s=0.7071$, in present Boolean model. In this way, in LGA simulation a pressure gradient can only be created associated to a density gradient, which must be small, assuring $M \ll 1$ and avoiding compressibility effects.

Three-dimensional representations of porous structure were obtained from two-dimensional sections by using Liang *et al.* (1998) reconstruction method. Reconstruction is based on a truncated gaussian stochastic simulation that preserves the first two moments of phase-function $Z(\mathbf{r})$, i.e., porosity ε and auto-covariance function $R_Z(u)$.

For simulating flow, present scheme uses periodic conditions and a *pumping zone* at the beginning of the domain (Figure 2.1). Periodic conditions assure that particles that escape from the end of lattice-domain are re-introduced at its beginning. In *pumping zone*, momentum is added to the particles, forcing them to the flow domain. In this way, model tries to mimic the real conditions related to a *real* hydraulic closed looping.

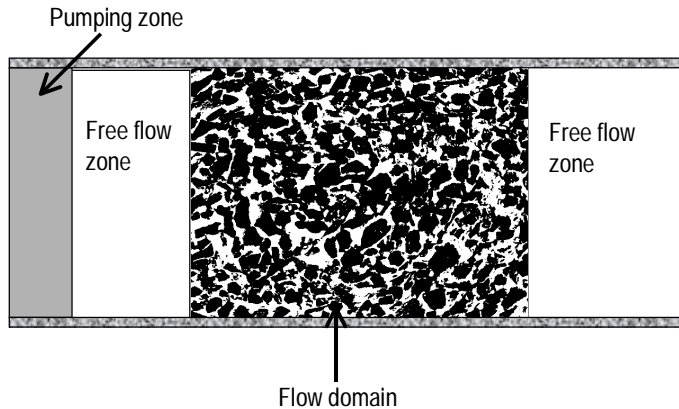
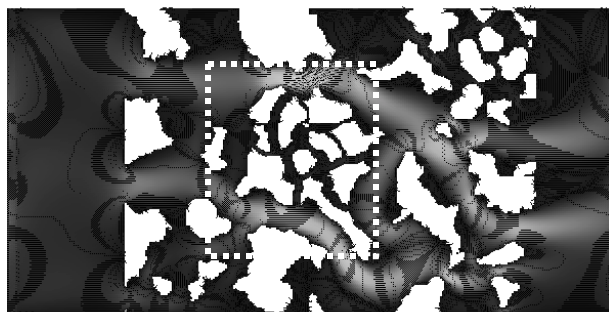


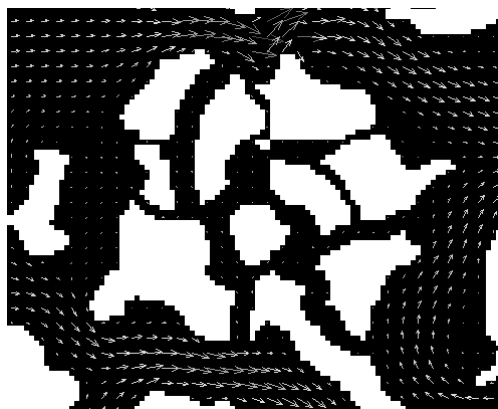
Figure 3.1. LGA simulation scheme.

2.4.2 Simulation process, computer requirements

Figure 2.2 presents a LGA flow simulation through an artificially constructed , two-dimensional, porous structure, with two main pore-scales. Although pore-space is connected in both scales, fluid flows, preferentially, through the larger scale space, circulating around the porous grains and creating stagnant and/or vortex flows inside the lower pore-scale space.



(a)



(b)

Figure 2.2. LGA flow simulation through an artificially constructed, two-dimensional, porous structure, with two main pore-scales: a) lighter gray is related to higher velocity modulus; b) zoom view showing circulation around the porous grains and stagnant and/or vortex flows inside the lower pore-scale space: velocity is represented by arrows

Figure 2.3 presents a typical simulation result, showing permeability evolution for a 300^3 representation of a sandstone, with a reported experimental permeability of 69 mD. Simulation starts from zero-velocity initial conditions and is established after, around, 15000 time steps.

LGA model has intrinsic fluctuations due to Boolean occupation of a discrete lattice with a finite number of directions. In this way, mean flow rate was evaluated, at each time step, by considering all the sites located inside the porous domain and time fluctuations were reduced by performing time averages. Figure shows simulation results for time averages, using, respectively, 100, 200, 400, 800 and 1600 time steps.

Collision table takes 65Mb of computer resident memory, independently of 3D representation size. A 32 bits variable is used for describing the micro-state $n_i(X,T)$ of each site. Process takes, around, 1Mb for storing the binary representation, 64 Mb for storing the micro-states, needing a total of 130 Mb for simulating a 200^3 representation. In this way, it was possible to run the most part of processes on ordinary Pentium processors. A 1 GHz processor takes about $2 \mu\text{s}$ to accomplish a single time-step, for each site. As collision and propagation steps are, only, performed on the sites located in porous phase, processing-time is, about, 3s for a 200^3 representation for a single time step and 12 h for 15000 time steps.

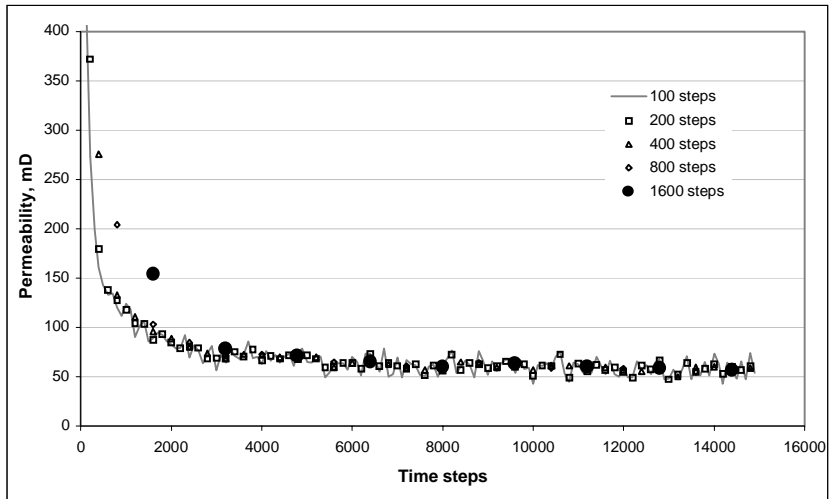


Figure 2.3. LGA permeability calculation for d18-connected 300^3 three-dimensional representation of a rock sample, using different time steps averaging. Experimental permeability value is 69 mD.

3. LATTICE-BOLTZMANN MESOSCALE MODELS

Lattice-Boltzmann (LB) are mesoscopic models, firstly introduced as a numerical *method* to solve Navier-Stokes equations (McNamara & Zanetti, 1988): Navier-Stokes equations are simulated at a mesoscopic level and mesoscopic lattice evolution follows a lattice equation (the *Lattice-Boltzmann equation*), written in the manner so as to retrieve Navier-Stokes equations at macroscopic level. In its first generation, LB models were only able to describe incompressible isothermal flows. A main contribution to LB theory was given by He & Luo (1997), who introduced an *a priori* procedure to systematically derive Lattice-Boltzmann models, with arbitrary precision, by using Gaussian-quadratures on continuum Maxwell-Boltzmann distribution.

Although very suitable from a computational point of view, the use of Boolean variables has very serious overcomes that may be summarized by considering: i) non-physical terms in macroscopic equations due to exclusion principle, ii) excessive noise,

produced by excessively drastic transitions and requiring spatial averages and iii) high transport coefficients.

In fact, considering that populations in the lattice b directions follow a Bernoulli distribution, it may be shown that, for scalar quantities, fluctuations σ in Boolean simulation are given by (see, also Boghosian *et al.*, 1997)

$$\sigma \sim \sqrt{\frac{1}{f m n}} \quad (3.1)$$

where f is the number of bits per site, m is the number of sites considered for spatial averages and n is the number of independent realizations.

Considering molecular-chaos hypothesis, mesoscale models start from the ensemble average of Boolean evolution equation, i.e., the lattice-Boltzmann equation (LBE) and proceeds actualizing distribution N_i at each \mathbf{X} , T in two simulation steps:

collision step

$$N'_i(\mathbf{X}, T) = N_i(\mathbf{X}, T) + \Omega_i(N_o, N_1, \dots, N_{b_m}), \quad (3.2)$$

propagation step

$$N_i(\mathbf{X} + \mathbf{c}_i, T+1) = N'_i(\mathbf{X}, T) \quad (3.3)$$

for $i=0, 1, \dots, b_m$.

It is easy to see that, although drastically reducing fluctuations, mesoscale models have the same remaining overcomes of Boolean models when collision term Ω_i is taken as the ensemble average of Boolean transitions (Eq. 2.5). Particularly, model would predict a non-physical Fermi-Dirac distribution at equilibrium, due to exclusion principle (McNamara and Zanetti, 1988).

Nevertheless, avoiding its Boolean nature, a collision model can be written for Ω_i with the condition that it leads to a physically consistent equilibrium distribution. In this way, Higuera and Jimenez (1989) proposed a linear approximation to Ω_i

$$\Omega_i(N_o, N_1, \dots, N_{b_m}) \sim \Omega_i(N_o^{eq}, N_1^{eq}, \dots, N_{b_m}^{eq}) + \sum_{k=0}^{b_m} \Lambda_{ik} (N_k^{eq} - N_k) \quad (3.4)$$

which reduces to BGK collision term (Bhatnagar *et al.*, 1954) when

$$\Lambda_{ik} = \frac{1}{\tau} \delta_{ik} \quad (3.5)$$

giving a *single* relaxation time model, Chen *et al.* (1991.c), Qian *et al.* (1992). Recently, He and Luo (1997), demonstrated that BGK relaxation equation

$$N_i(\mathbf{X} + \mathbf{c}_i, T+1) - N'_i(\mathbf{X}, T) = \frac{N_i^{eq} - N_i}{\tau} \quad (3.6)$$

can be deduced from its well-known counterpart BGK equation from continuous kinetic theory, by using a discrete set of velocities.

In Eq. (3.6), a 2nd order velocity polynomial form is given to equilibrium distribution, which coefficients are obtained by considered lattice isotropy and by requiring

$$\rho = \sum_{i=1}^{b_m} N_i^{\text{eq}} + N_o^{\text{eq}} \mathbf{b}_r \quad (3.7)$$

$$\mathbf{u} = \frac{1}{\rho} \sum_{i=1}^{b_m} N_i^{\text{eq}} \mathbf{c}_i \quad (3.8)$$

$$\Pi_{\alpha\beta} = \sum_{i=1}^{b_m} N_i^{\text{eq}} c_{i\alpha} c_{i\beta} = c_s^2 \rho \delta_{\alpha\beta} + \rho u_\alpha u_\beta \quad (3.9)$$

Considering these requirements, it may be shown that

$$N_i^{\text{eq}} = \frac{\rho}{b} + \frac{D}{b_m c^2} c_{i\alpha} \rho u_\alpha + \frac{D(D+2)}{2b_m c^4} c_{i\alpha} c_{i\beta} \rho u_\alpha u_\beta - \frac{D}{2b_m c^2} \rho u^2 \quad (3.10)$$

$$N_o^{\text{eq}} = \frac{\rho}{b} + \frac{1}{b_r c^2} \rho u^2 \quad (3.11)$$

A Chapman-Enskog analysis for the model above described shows that correct Navier-Stokes equations are retrieved for non-compressible flows. In fact, non-physical compressible effects appear, proportional to M^2 , in momentum equation for compressible flows.

3.1 Thermodynamic consistent mesoscale models

To give thermodynamic consistency, lattice models must consider energy relaxation. A pioneer work on a 2D thermal lattice BGK model was published by Alexander *et al.* (1993), generalized by McNamara & Alder. (1993) to include different relaxation times for the stress and energy. Chen Oashi and Akiyama. (1994) used a 4th-order velocity expansion for the equilibrium distribution, up-grading the lattice symmetry to ensure isotropy for the sixth-rank velocity-moment tensor, using a single relaxation time model,

$$N_i(\mathbf{X} + \mathbf{c}_{ik}, T+1) - N_{ik}(\mathbf{X}, T) = \frac{N_{ik}^{\text{eq}} - N_{ik}}{\tau}, \quad (3.12)$$

where k designates an energy level for velocity vector \mathbf{c}_{ik} , giving the modulus of \mathbf{c}_{ik} . Equilibrium distribution was written as

$$N_{ik}^{\text{eq}} = A_k + M_k c_{ik,\alpha} u_\alpha + G_k u^2 + J_k (c_{ik,\alpha} u_\alpha)^2 + Q_k (c_{ik,\alpha} u_\alpha) u^2 + H_k (c_{ik,\alpha} u_\alpha)^3 + R_k (c_{ik,\alpha} u_\alpha)^2 u^2 + S_k u^4. \quad (3.13)$$

Chen and co-workers model retrieves the correct thermo-hydrodynamic equations for compressible flows, with the only, visible limitation in the Prandtl number due to the use of a *single* relaxation time.

3.2 Sample application: vortex shedding from 2D obstacles

Boundary conditions at solid surfaces were simulated by using the bounce-back condition

$$N_{-i}(\mathbf{X}_b, T+1) = N_i(\mathbf{X}_b, T),$$

for a boundary site X_b in the fluid, when direction i points to the solid surface. This assures the adherence condition $u=0$ at the boundary.

When N_i particles are reflected back at boundary sites X_b , they exchange the momentum $2N_i c_i$ with the solid surface, since lattice-Boltzmann particles have unitary mass. Considering that this exchange is performed in each unitary time step, this momentum exchanged represents a force F_i , on the solid surface adjacent to site X_b . In this way, the total force on the solid body can be calculated by.

$$\mathbf{F} = \sum_{X_b} \sum_i \mathbf{F}_i(X_b).$$

In this way, the drag and the lift force can be calculated without the need of cumbersome numerical derivatives of the flow velocity field at the solid boundary.

Figures 3.1-3.2 show sample results for a single circular cylinder. Flow is laminar and vortex shedding is very stable for Re smaller than 47.5 (Figure 3.1). For larger Re , small flow perturbations gives rise to vortex release from the cylinder, starting flow transition. Vortex formation frequencies can be measured by calculating the Fourier transform of the lift force.

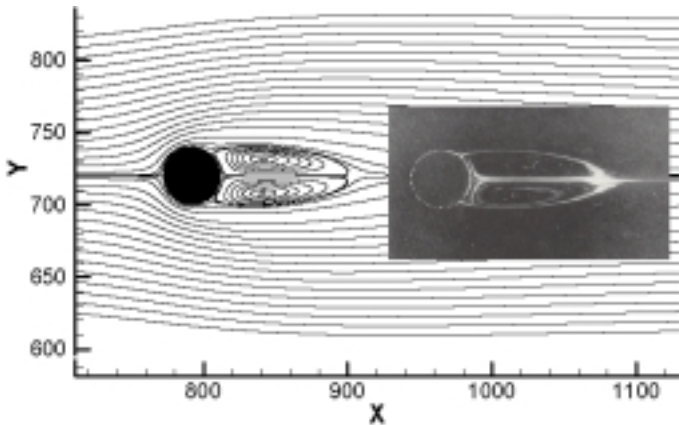


Figure 3.1 Comparison of streamlines from LB simulation for laminar flow around a circular cylinder with experimental visualization (Tritton, 1988) at $Re=40$.

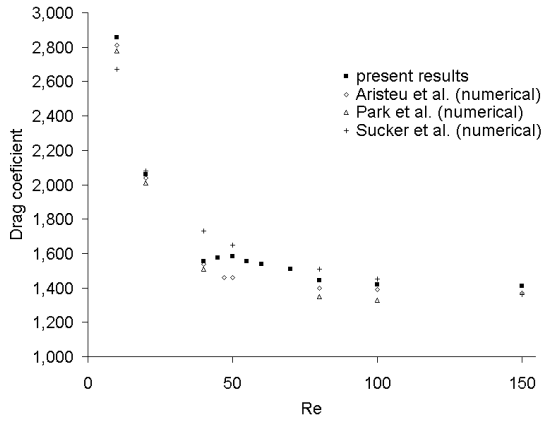


Figure 3.2. Comparison of LB calculated drag coefficient with others authors for a circular cylinder.

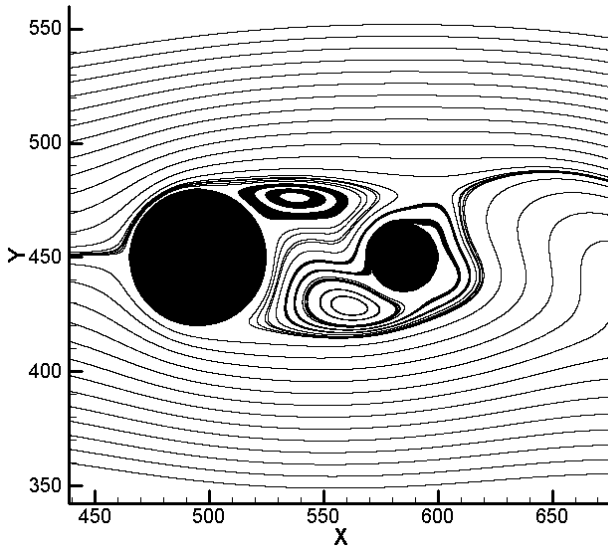


Figure 3.3. Sample streamlines for the vortex shedding from two circular cylinders in tandem at $Re=200$. The centers of the two cylinders are separated by $L=1.5d$, where d is the diameter of the left cylinder. Right cylinder has a diameter $D=d/2$.

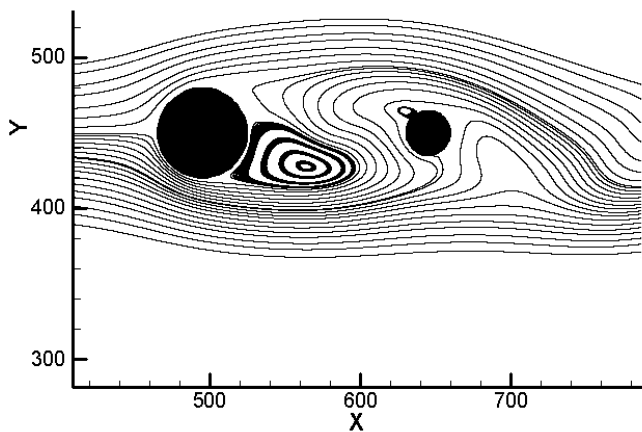


Figure 3.4. Sample streamlines for the vortex shedding from two circular cylinders in tandem at $Re=200$. The centers of the two cylinders are separated by $L=2.5d$, where d is the diameter of the left cylinder. Right cylinder has a diameter $D=d/2$.

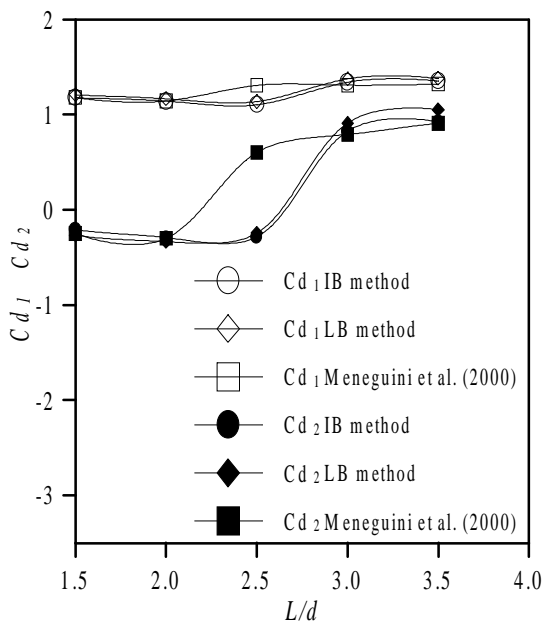


Figure 3.5. Drag coefficient for the vortex shedding from two circular cylinders in tandem at $Re=200$. d is the diameter of the left cylinder. Right cylinder has a diameter $D=d/2$ (Lima & Silva *et al.*, 2002).

A comparative work between lattice-Boltzmann and immersed boundary method was undertaken by Lima & Silva *et al.* (2002) for the analysis of vortex shedding around two circular cylinders in tandem, for $Re=200$. This is a very interesting problem, since when the two cylinders are close enough, the vortex generated at the intermediate region are not released to the outer flow and drag force is negative for the second cylinder. Results are shown in Figures 3.3-3.5. Agreement between lattice Boltzmann and immersed boundary is almost perfect and transition to positive drag is predicted at $L \sim 2.6d$ by both methods (L is the distance between the centers of the two cylinders).

4. MULTI-BITS AND INTEGERS MODELS

Boltzmann models suffer from stability problems that are common to all numerical methods based on floating-point arithmetics and restricting Courant-Lewis-Friedrich number working range (Rothman & Zaleski, 1997). Boolean models have as its more serious drawbacks: i) the prediction of macroscopic non-physical effects due to the exclusion principle and ii) the excessively high noise, requiring spatial and time averages. Multi-bits and integers models are presently being developed with the purpose of reducing these inconvenients.

Models are based on the idea of filling each lattice direction i with an arbitrary number of distinguishable (multi-bits) or undistinguishable (integers) bits (Bhogosian *et al.*, 1997). In this way,

$$s = (s_{01}, \dots, s_{0b_r}; s_{11}, \dots, s_{b_m 1}; \dots; s_{1\ell}, \dots, s_{b_m \ell})$$

represent a microscopic state s of a multi-bits model, where for each i, j , s_{ij} is a Boolean variable, b_r is the allowable number of undistinguishable rest particles and particles occupation proceeds along the b_m directions of each of identical P -planes, which are ℓ repeated. For 2D simulations each P -plane can be considered as a 2D hexagonal lattice obtained by considering for each site \mathbf{X} , the first 6 neighbors at 1 lattice-unit from \mathbf{X} , the second 6 neighbors at $\sqrt{3}$ lattice units from \mathbf{X} and so on. In this way, particle speeds can be $1, 3^{1/2}, 2, 7^{1/2}, \dots$ (Grosfils, Boon, Lallemand, 1992)

Considering $n_{ij}(\mathbf{X}, T)$ to be the Boolean variable related to i -direction particle occupation at j -plane of site \mathbf{X} , at time T , microscopic dynamics follows,

$$n_{ij}(\mathbf{X} + \mathbf{c}_i, T + 1) - n_{ij}(\mathbf{X}, T) = \omega_{ij}(n_{01}, \dots, n_{0b_r}; n_{11}, \dots, n_{b_m 1}; \dots; n_{1\ell}, \dots, n_{b_m \ell})$$

where ω_{ij} is the full collision term, written as,

$$\omega_{ij} = \sum_{s, s'} \alpha_{\xi(\mathbf{X}, T)}(s, s') (s'_{ij} - s_{ij}) \prod_k n_{0k}^{s_{0k}} (1 - n_{0k})^{1 - s_{0k}} \prod_m \prod_p n_{pm}^{s_{pm}} (1 - n_{pm})^{1 - s_{pm}}$$

where $\xi(\mathbf{X}, T)$ is a random number attributed to site \mathbf{X} , at time T

Collisions are performed preserving mass, ρ , momentum, ρu and kinetic energy, ε ,

$$\rho = \sum_{ik} n_{ik}$$

$$\rho \mathbf{u} = \sum_{ik} n_{ik} \mathbf{c}_i$$

$$\rho \varepsilon = \frac{1}{2} \sum_{ik} n_{ik} c_i^2$$

Furthermore, collision rules are required to satisfy semi-detailed balance. Main limitation of multi-bits models is related to the excessively large computer resident memory required to store the collision table. In this way, two planes of a FCHC model with 24 directions require 10^6 Mb of resident memory.

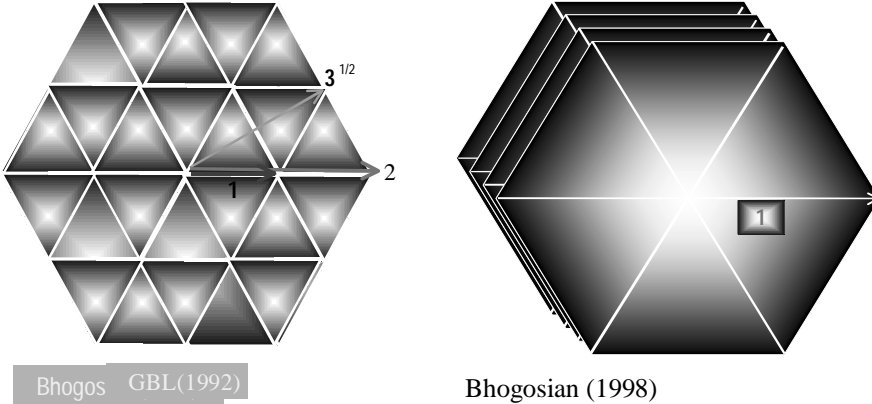


Figure 4.1 GBL multi-speed model and Bhogosian integers models

5. BOOLEAN MODEL FOR MISCIBLE AND IMMISCIBLE FLUIDS

Mixtures and diffusion processes were simulated, Rothman and Zaleski (1997), by distinguishing different kinds p of particles. Most common models use two-bit Boolean variables (r_i , b_i) representing colored particles of identical mass, like red ($p=r$) and blue ($p=b$) and diffusion coefficient can be related to collisions frequency between particles of different colors.

Long-range attraction between particles of the same kind promotes particles separation, being responsible for interfacial tension. Boolean models for simulating immiscible fluids flow were, firstly, proposed by Rothman and Keller (1988). In this model, long range attraction between particles of the same kind is modeled by modifying the collision step, introducing an additional *separation* step between particles of different kinds, based on the information of the populations in the *first neighbors* of site \mathbf{X} , in time step T . Output site configuration is decided after a maximization step for the color flux, in accordance with a color gradient at site \mathbf{X} .

Rothman and Keller's model is computer expensive when processing time needs are considered. Chen and co-workers (Chen *et al.*, 1991.a) proposed a two-bits local model, where the neighbors survey of Rothman and Keller was avoided, by introducing *colored holes*. Colored holes are null-mass particles representing the *memory* of the kind of a given particle, and moves in the same direction that particle moved before collision. The state of a given site is represented by a *two-bit* variable. In this way, in separation step, particles are deviated to the direction from where holes were originated, simulating *long range attraction*, by using, only, *local* rules. This is achieved by *maximizing* the color flux in a given site \mathbf{X} . Nevertheless, Chen's optimization step is, also, computer expensive with respect to processing time.

A four-bit model is presented bellow based on Santos (2000), Santos & Philippi (a) (2002) and Santos *et al.*(b) (2002). Intended to model the flow of immiscible fluids, the first two bits are used for different kinds r and b of particles, whereas the remaining two-bits are used for, respectively, r and b mediators. When a site \mathbf{X} can be considered as an attractive center for p particles, $p=r, b$, it will emit mediators of kind p that will be propagated to neighbor sites, in propagation step. Interference of p -mediators pull back p -particles to site \mathbf{X} , moving away from \mathbf{X} . In this way, mediators try to simulate the effect of long-range forces on fluid separation, following very simple emission and interference rules,.

The state of a given site \mathbf{X} at time T is given by a four-bit Boolean variable ($r_i(\mathbf{X}, T)$, $b_i(\mathbf{X}, T)$, $m_i^r(\mathbf{X}, T)$, $m_i^b(\mathbf{X}, T)$), $i=1, \dots, b$. where r , b , m^r and m^b belongs to $\{0,1\}$ and designate, respectively, r particles, b particles, r mediators and b mediators. Model allows simultaneous r_i and b_i bit occupation, but exclusion principle is maintained between particles of the same kind. Particles are considered to have the same, unitary, mass and mediators are null-mass particles propagating field information at lattice speed c .

Microdynamics has the following steps:

i) *Collision*. Collisions are responsible for mixing particles of different kinds, in the transition region, being related to binary species diffusion coefficient D_{rb} . In a discrete lattice gas space, microdynamics equation relating post-collision Boolean variable p_i' to p_i can be written as

$$\begin{aligned} p_i'(\mathbf{X}, T) - p_i(\mathbf{X}, T) &= \omega_i^p(r_1, \dots, r_b, b_1, \dots, b_b) \\ &\equiv \omega_i^p(r^*(\mathbf{X}, T), b^*(\mathbf{X}, T)), \end{aligned} \quad (5.1)$$

where $p^* = (p_1, \dots, p_b)$ designates a pre-collision configuration for p particles on site \mathbf{X} , at time T , sequence $1, \dots, b$ is related to Boolean occupation for b allowable particles in a lattice with b directions. A Boolean variable with $2b$ bits, is used to designate an arbitrary particle state $s = (s_1^r, \dots, s_b^r, s_1^b, \dots, s_b^b)$ of the lattice model in the Cartesian product $B_r \times B_b$ space. Collision operator,

$$\begin{aligned} \omega_i^p : B_r \times B_b &\rightarrow \{-1, 0, 1\} \\ (r^*, b^*) &\rightarrow \omega_i^p(r^*, b^*), \end{aligned} \quad p=r, b \quad (5.2)$$

$\forall i=1, \dots, b$, maps a 2^{2b} dimensional space on the set $\{-1, 0, 1\}$ and can be written as

$$\omega_i^p(r^*, b^*) = \sum_{s, s'} \alpha_\xi(s, s') (s_i^{p'} - s_i^p) \prod_j r_j^{s_j^r} (1 - r_j)^{1-s_j^r} b_j^{s_j^b} (1 - b_j)^{1-s_j^b}, \quad (5.3)$$

where $\alpha_\xi(s, s')$ is the transition matrix (Rothman and Zaleski, 1997), $\xi = \xi(\mathbf{X}, T)$ is a random variable attributed to site \mathbf{X} , at time T . Transition matrix must assure mass and momentum conservation in collisions. In addition, $A(s, s') = \langle \alpha_\xi(s, s') \rangle$ must satisfy the semi-detailed balance condition:

$$\sum_{s'} A(s, s') = \sum_s A(s, s') = 1, \quad (5.4)$$

as sufficient conditions for satisfying H-Theorem in describing irreversibility of diffusion processes (Frisch *et al.*, 1986).

ii) *Interference with field mediators.* After collision, particles of kind p , in the site \mathbf{X} , are subjected to long-range attraction from particles of the same kind. In present model, this is simulated locally, by inverting the momentum of each p -particle when a) it finds a p -mediator in the same direction and b) opposite direction is free from p -particles (since exclusion principle is preserved when particles are of the same kind). In this way, in comparison with Chen *et al.*'s model (Chen *et al.*, 1991a), although momentum is not, *locally*, preserved, this rule enable avoiding Chen *et al.* computer expensive optimization step and is of no-consequence for the global behavior of the model, when a sufficiently great number of realizations are considered.

iii) *Emission of field mediators.* Considering an elementary volume ϑ located inside a mixture of two real gases, ϑ acts an attractive center for p molecules when n_p/n is above some critical value $(n_p/n)^*$, with a potential strength that depends on the kind of r - r , b - b and, consequently, r - b , interactions. In present LGA model, site \mathbf{X} will be a source of p mediators when $(n_p/n) > (n_p/n)^*$, with a given emission probability P_e that depends on particle- p concentration n_p/n on site \mathbf{X} , at time T . Emission probability is, thus, related to the potential strength in the transition region, giving the interfacial tension, σ_{rb} . When $P_e=0$, independently of n_p/n , fluids r and b will mix without long-range field restriction.

iv) *Extinction of field mediators.* In addition to field strength, interaction length is an important parameter, contributing to transition layer thickness. In present model, interaction length is related to an extinction probability P_a . Thus, for a field mediator $m_p(\mathbf{X}, T)$ to be annihilated two conditions are imposed: a) $n_p(\mathbf{X}, T)=0$ at site \mathbf{X} and b) $P(\mathbf{X}, T) \leq P_a$, where P is a random variable attributed to site \mathbf{X} , at time T , $0 \leq P \leq 1$. These conditions assure that, e.g., a field mediator r will be never destroyed in the transition region r - b and that r -mediators will be found inside b -phase, trying to rescue r -particles moved to b -phase by collisions.

v) *Propagation.* In propagation, particles and mediators are propagated to next neighbors, in the same manner as in conventional LGA models (Rothman and Zaleski, 1997). In present model, propagation of p -mediators in the i -direction will pull back p -particles to site \mathbf{X} , from neighbors sites $\mathbf{X} + \chi \mathbf{e}_i$, with decreasing probabilities that depend on emission and annihilation probabilities and on distance χ from site \mathbf{X} (Santos, 2000).

vi) *Boundary conditions.* Wetting/non-wetting properties of a pair of fluids with respect to solid surfaces are a macroscopic result of differential, long-range attraction between solid and fluid molecules. At *equilibrium*, this preferential attraction can be summarized by the formation of a well defined contact angle, θ , between fluid interface and the solid wall, which depends on the pair of fluids and on the solid surface. In present

model, preferential attraction of solid wall S, with respect to a given fluid p, is simulated by reflecting back p-mediators at boundary sites X_s , with a given probability P_s , related to θ . Non-wetting fluid mediators are not reflected at boundary sites, being annihilated at these sites. This condition may be written as,

$$m_i^p(X_s, T+1) = \begin{cases} m_{-i}^{p*}(X_s, T) & \text{when } P(X_s, T) \leq P_s \\ 0 & \text{otherwise} \end{cases} \quad (5.5)$$

$\forall i$ pointing outward the solid surface, when p is the wetting fluid with respect to solid surface and where P is a random variable attributed to site X_s , at time T, $0 \leq P \leq 1$.

vii) *External forces: forcing step.* Forcing step is performed before collision step, above described. Labeling by k the lattice direction parallel to external field direction, external forces \mathbf{g}_p are simulated by reversing the momentum of particles r and b, located at direction -k opposed to \mathbf{g}_p , when direction, k, is free from particles of the same kind. Probability $P_{g,p}$ to this reversion, represents the force strength \mathbf{g}_p on component p. Microdynamic equation describing *forcing step* can be written as:

$$p_k^i(X, T) = \begin{cases} p_{-k}(X, T)(1 - p_k(X, T)) & \text{when } P(X, T) \leq P_{g,p} \\ p_k & \text{otherwise} \end{cases} \quad p=r, b \quad (5.6)$$

where $P(X, T)$ is a random variable attributed to site X, at time T, $0 \leq P \leq 1$.

At equilibrium, using ergodic hypothesis when considering the whole lattice domain, the mean effect of forcing step on p-particles can be calculated by,

$$\mathbf{f}_p = 2P_{g,p} \frac{\langle n_p \rangle}{b_t} \left(1 - \frac{\langle n_p \rangle}{b_t} \right) \mathbf{c}_k, \quad (5.7)$$

which is the force, related to the momentum the $\langle n_p \rangle$ particles per site are expected to gain in direction k during a lattice time-step.

5.1 Sample application: Droplet formation under gravity action: Santos (2000), Santos & Philippi (a) (2002)

Although very interesting from a physical point of view, droplet formation from a dropper is a very difficult problem, when we consider classical discrete methods of fluid mechanics. Droplet formation is pictured in Figure 1.2.

From a macroscopic point of view droplet's shape time evolution is linked to the competition it is subjected between gravity action, viscosity of the droplet fluid and interfacial tension. In this way, interfacial forces hold the droplet until break-off, as droplet weight increases. Break-off starts with the development of a throat, which becomes thinner in time and from where droplet fluid is pulled downward against the droplet and redistributed horizontally by viscous forces, giving an almost ellipsoidal shape to the falling droplet, with a major axis oriented along horizontal direction.

From a microscopic point of view, during the first moments of droplet fall, r-particles at droplet surface are subjected to long-range forces from r-phase inside the dropper,

maintaining the integrity of r-phase in despite of gravity action. Droplet break-off starts when combined action of gravity and downward long range attraction from the created droplet increases with respect to upward long range attraction from r-phase inside the dropper, giving raise to the formation of droplet throat. During and after break-off, r-particles in the throat are pulled against the droplet, where these particles are redistributed inside the droplet by *r-r collisions* (related to the viscosity of droplet fluid).

Figure 5.1 shows a sequence of simulation results using present field-mediators model. Comparison of Figures 5.1 and 1.2 shows a very good qualitative agreement between simulation and experimental results.

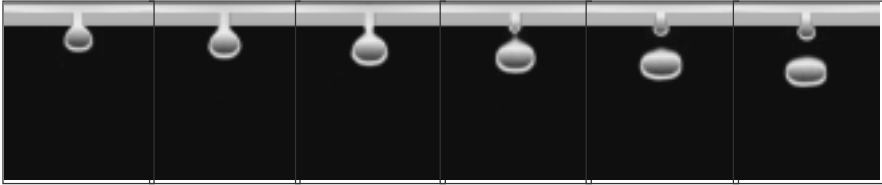


Figure 5.1 Simulation of droplet formation under gravity action.

5.2 Sample application: spreading of a liquid drop on a flat surface (Wolf *et al.*, 2002 and Wolf, 2002).

Fig. 5.2 shows Boolean simulation results for the spreading problem arising when a liquid drop is put in contact with a flat solid surface, until mechanical equilibrium is reached and drop surface establishes a definite contact angle with the solid surface. Long-range attraction between solid surface and liquid phase is simulated by using surface mediators that are created at the solid boundary sites and pull liquid phase particles to the solid surface. Surface mediators are created with an emission probability P_e^s , related to the interaction potential strength and annihilated with an annihilation probability P_s^a , to be associated with the interaction length. These microscopic parameters can be controlled to give the desired equilibrium contact angle, corresponding to a given pair of fluids in contact with a solid surface.



Figure 5.2 Spreading of a liquid drop on a flat surface

Simulation predicts a power-law behavior, $R \propto t^n$, for the time evolution of the radius of the wetted solid surface with time, where $n=0.33$. This agrees with several experimental visualization results, although exponent 'n' is much dependent on the initial configuration of the liquid drop.

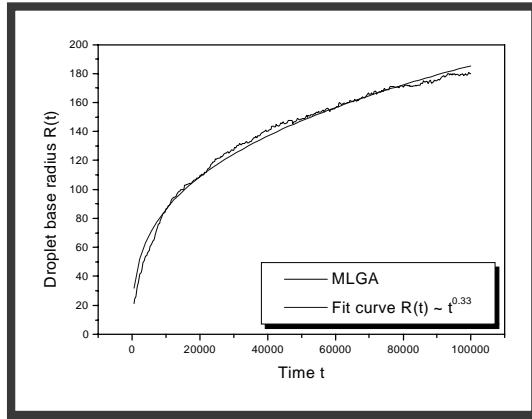


Figure 5.2 Time evolution of wetted surface radius

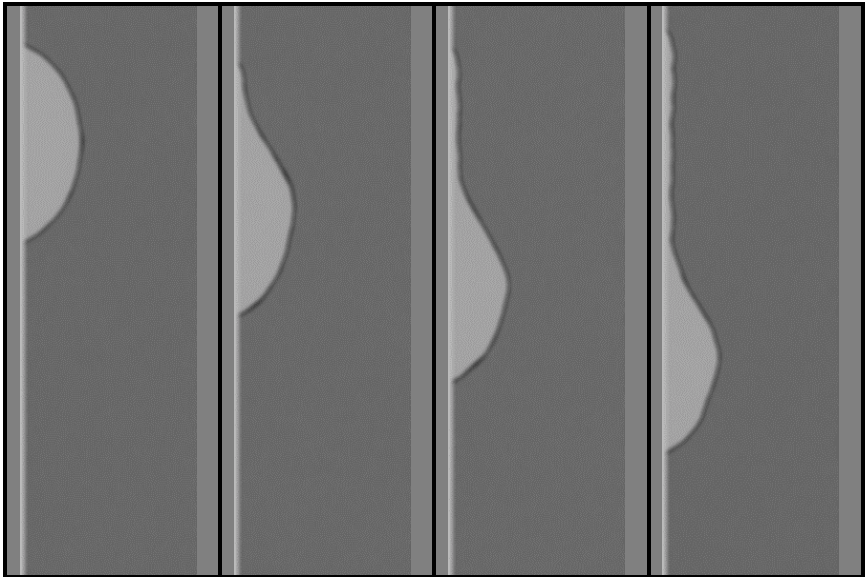


Figure 5.3 Spreading of a liquid drop on a vertical surface under gravity action.

Figure 5.3 shows the simulation results for the spreading of a liquid drop on a flat vertical surface under gravity action.

6. A BOLTZMANN MODEL FOR MISCIBLE FLUIDS (Facin, 2002, Facin *et al.*, 2002)

At a given site, in a mixture of two fluids r and b, transition term can be written as a sum of two relaxation terms. Collisions between particles of the kind r, try to impose equilibrium distribution $R_{i,r}^o = R_i^o(\rho_r, \mathbf{u}_r)$, with a relaxation time τ_r , specific to kind r particles and related to r-fluid viscosity. Collisions between particles of kind b, try to impose a *different* equilibrium distribution, with a relaxation time τ_b . Collisions between particles r and b try to impose a common distribution to both kinds of particles $R_{i,rb}^o = R_i^o(\rho_r, \mathbf{u}_b)$ with a relaxation time τ_{rb} , related to binary species diffusion coefficient. In this way,

$$\Omega_i^r = \omega_r \frac{R_{i,r}^o(\rho_r, \mathbf{u}_r) - R_i}{\tau_r} + \omega_b \frac{R_{i,rb}^o(\rho_r, \mathbf{u}_b) - R_i}{\tau_{rb}} \quad (6.1)$$

for $i=0,1,\dots,b_m$, where $\omega_r = \rho_r / \rho$ and $\omega_b = \rho_b / \rho$.

Equilibrium distribution for pure fluid r is, usually, required to satisfy:

- i) mass conservation of r and b particles

$$\sum_{i=1}^{b_m} R_i + R_0 b_r = \rho_r \quad (6.2)$$

- ii) momentum conservation

$$\sum_{i=1}^{b_m} R_i \mathbf{c}_i = \rho_r \mathbf{u}_r \quad (6.3)$$

- iii) preservation of momentum flux at zero-th order

$$\Pi_{\alpha\beta}^r = \rho_r u_{r\alpha} u_{r\beta} + \frac{b_m c^2}{bD} \rho_r \quad (6.4)$$

Collisions of r and b particles are required to satisfy:

- i) mass conservation of r and b particles

$$\sum_{i=1}^{b_m} R_{i,rb} + R_{o,rb} b_r = \rho_r \quad \sum_{i=1}^{b_m} B_{i,rb} + B_{o,rb} b_r = \rho_b \quad (6.5)$$

ii) momentum conservation

$$\sum_{i=1}^{b_m} R_i \mathbf{c}_i + \sum_{i=1}^{b_m} B_i \mathbf{c}_i = \rho \mathbf{u} \quad (6.6)$$

iii) preservation of momentum flux at zero-th order

$$\Pi_{\alpha\beta} = \rho u_\alpha u_\beta + \frac{b_m c^2}{bD} \rho \quad (6.7)$$

7. A BOLTZMANN MODEL BASED ON MEDIATORS FOR IMMISCIBLE FLUIDS (IMLB): Santos & Philippi (a) (2002), Facin (2002), Facin *et al.* (2002)

Boltzmann models have been developed for immiscible fluids by Gustensen *et al.* (1991), Shan and Chen (1994) and by Martys and Chen (1996). In the following, the main idea of Santos & Philippi (a) (2000), considering mediators for modeling long-range forces is used for Boltzmann mesoscopic models.

When fluids are immiscible, long-range attraction between particles of the same kind, will try to separate the two fluids. In this way, in addition to r-r and r-b collisions in the transition layer, there will be a separation effect due to long-range fields.

In its simplest form, the probability of finding red mediators on a given site \mathbf{X} , at time T , $M_i^r(\mathbf{X}, T)$ can be written, in emission step, as proportional to $\rho_r(\mathbf{X}, T)$. This information is propagated to next neighbors sites, where interference is to be produced. The presence of a long-range field from r-particles in a given site \mathbf{X} is related to a non-null value of mediators distributions $M_i^r(\mathbf{X}, T)$ and $M_i^b(\mathbf{X}, T)$ and their action will try to move red particles to the direction from where red mediators came and blue particles to the direction from where blue mediators came. In this way, we can define a separation velocity,

$$\mathbf{u}_m = \sum_{i=1}^{b_m} (M_i^r - M_i^b) \mathbf{c}_i \quad (7.1)$$

and collision operator can be written as

$$\Omega_i^r = \omega_r \frac{R_{i,r}^o(\rho_r, \mathbf{u}_r) - R_i}{\tau_r} + \omega_b \frac{R_i^o(\rho_r, \mathbf{u}_b^m) - R_i}{\tau_{rb}} \quad (7.2)$$

where

$$\mathbf{u}_b^m = \mathbf{u}_b - A \hat{\mathbf{u}}_m \quad (7.3)$$

In the above equation, $\hat{\mathbf{u}}_m$ is the normalized separation velocity \mathbf{u}_m . Coefficient A gives the long-range potential strenght and will be related to interfacial tension σ_b between fluids r and b . When $A=0$, the model reduces to the miscible collision term, given by Eq. (6.1). It

has been shown that above collision model satisfies all the restrictions imposed by the conservation laws. Furthermore, up-scaling to macroscopic scale shows that presently proposed model gives a consistent hydrodynamic behavior, for incompressible fluids (Facin, 2002).

7.1 Sample application: bubble ascension dynamics, under gravity action (Philippi *et al.*, 2001)

Figure-7.1 shows results of a two-dimensional simulation for bubble ascension against gravity. Simulation domain is 400X800. and bubble is considered as a circle at $t=0$, with an initial diameter of 100 lattice-units. Simulation uses a 2D FCHC lattice. Very interesting dynamical effects produce bubble deformation during ascension.

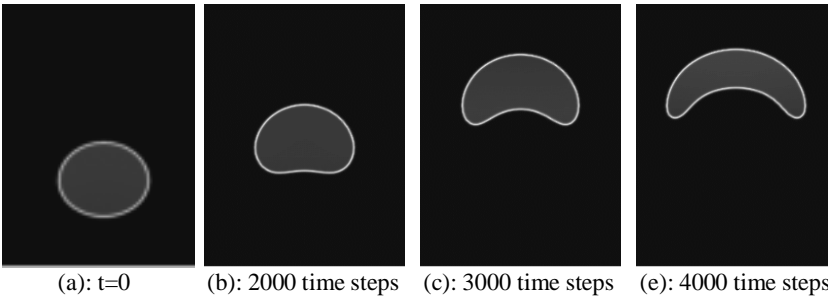


Figure 7.1. Bubble ascension against gravity. Simulation domain is 400 x 800. Initial bubble diameter corresponds to 100 lattice units.

7.2 Sample application: pore invasion by a wetting fluid: Santos & Philippi (b), (2002)

Figure 7.2 illustrates the simulation results obtained with IMLB, when a wetting fluid invades a 2D pore with a rather complicated geometry. Pressure is identical at the two outside chambers and invasion proceeds by capillary forces, only. When wetting fluid exits the first throat, the interface curvature radius is increased and interface speed is reduced. Interface moves very slowly in this phase (b), until attractive forces between the wetting fluid and the opposite solid surface produce the resident non-wetting fluid break-off (c). From this point, the wetting fluid moves very fast along the two channels and non-wetting fluid is displaced in a piston-like process (d). Displacement rate is, again, reduced when wetting fluid enters the right, internal chamber (e). In this phase attractive forces between the interface and the pore surface, at the bottom of the cavity, can produce non-wetting fluid entrapment.

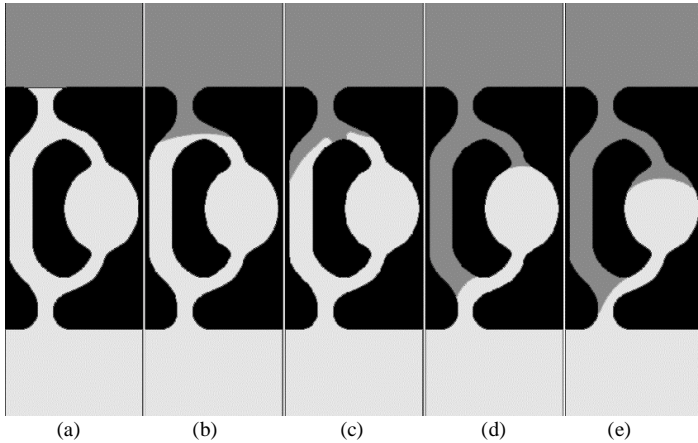


Figure 7.2 Break-off and piston-like displacement in wetting fluid invasion

8. CONCLUSIONS

Lattice gas automata concepts appear to be very suitable for explaining *complex* macroscopic effects, based on *simple* models of fluid behavior at molecular level.

In this lecture, Boolean and Boltzmann models were presented for simulating single-phase flows and the flow of immiscible fluids. Single phase flow through porous media was presented in details, using a Boolean model for predicting intrinsic permeability of porous rocks reconstructed from two-dimensional petrography thin-plates. Vortex shedding was simulated using a lattice Boltzmann model, appropriated to incompressible, but arbitrary Reynolds number, flows. Main ideas related to some improvements of Boolean models, by filling the lattice directions with an arbitrary number of bits are, also, presented. Field mediators were introduced, for representing the action of long-range fields when modeling immiscible fluids in the study of complex physical phenomena such as coalescence and fragmentation.

Considering their inherent simplicity, presented results, apparently, confirm the adequacy of lattice gas models in the study of fluid flow and physical phenomena related to fluid flow that require lower-level description scales.

9. ACKNOWLEDGEMENTS

Prof. Sávio Leandro Bertoli, from FURB/SC has greatly contributed to our present state of knowledge on lattice-gas fundamentals and greatly enhanced our literature on this subject, during his doctoral work at our laboratory. Some results presented here were extracted from Fabiano Gilberto Wolf, MSc thesis and doctoral work. Prof. Paulo Cesar Facin, from UEPG/Pr has deeply contributed in the theoretical elucidation of immiscible fluids interface physics, during his Doctoral work. Eng. Marcos Cabral Damiani, from Engineering Software and Scientific Simulation (ESSS) has provided important simulation and visualization tools, significantly smoothing the progress of our research work. Authors also acknowledge the undergraduate students Luis Adolfo Hegele Jr. and Rodrigo Surmas.

10. REFERENCES

Historical references

- Bernoulli, D., 1738, *Hydrodynamica*, Argentoria, cited in Jeans, J. (1925) *Dynamical Theory of Gases*, 4th edition, Dover, New York.
- Bhatnagar P., Gross, E.P., Krook, M.K., *Phys. Rev.*, 94, 511 (1954).

Books

- Chapman, S., Cowling, T.G. (1970), *The Mathematical Theory of Non-Uniform Gases* (3rd Ed.), Cambridge University Press .
- Tritton, D. J. "Physical fluid dynamics". 2nd. ed. Oxford, Clarendon, 1988.
- Rothman, D. H., Zaleski, S. (1997). "Lattice-gas cellular automata: simple models of complex hydrodynamics" (Cambridge University Press).
- Rivet, J.P., Boon, J.P. (2001), "Lattice Gas Hydrodynamics", Cambridge University Press, Cambridge.

Basic papers on Boolean models

- Hardy, J., Pomeau, Y., Pazzis O., 1973, Time Evolution of a Two-Dimensional Model System. I. Invariant States and Time Correlation Functions, *J. Math. Phys.* 14, 1746-1759.
- Hardy, J., de Pazzis O.; Pomeau Y., 1976. Molecular dynamics of a classical lattice gas: Transport properties and time correlation functions, *Phys. Rev. A* 13, 1949-1961.
- Wolfram, S., 1983, Statistical Mechanics of Cellular Automata, *Reviews of Modern Physics* 55, 601-644.
- Wolfram, S., 1984, Cellular automata as models of complexity, *Nature* 311, 419.
- Wolfram, S., 1986 Cellular Automaton Fluids: Basic Theory, *J. Stat. Phys.* **45**, 471-526.
- Frisch, U., Hasslacher B., Pomeau Y. (1986). "Lattice-Gas Automata for the Navier-Stokes Equation" *Physical Review Letters* 56, 1505-1508.
- Frisch, U., d'Humières, D., Hasslacher, B., Lallemand, P., Pomeau, Y. and Rivet, J. (1987). "Lattice Gas Hydrodynamics in Two and Three Dimensions" *Complex Systems* 1, 649-707.
- d'Humières, D., Lallemand, P., and Frisch, U. (1986). "Lattice gas models for 3D hydrodynamics" *Europhys. Lett.* 2, 291-297.

Basic papers on lattice-Boltzmann equation

- McNamara G. G. and Zanetti G. (1988). "Use of the Boltzmann Equation to Simulate Lattice-Gas Automata" *Physical Review Letters* 61, 2332-2335.
- Higera, F. and Jimenez, J. (1989). "Boltzmann approach to lattice gas simulations." *Europhys. Lett.* 9, 663-668.
- Chen, S., Wang, Z., Shan, X., Doolen, G. (1991.c). "Lattice Boltzmann computational fluid dynamics in three-dimensions", *J. Stat. Phys.*, 68, 379-400.
- Qian, Y. H., d'Humières D., Lallemand P. (1992) "Lattice BGK Models for Navier-Stokes Equation" *Europhys. Lett.* 17, 479-484.

Thermodynamic consistent Boltzmann models

- Grosfils P, Boon JP, Lallemand P (1992), "Spontaneous fluctuation correlations in thermal lattice-gas automata", *Phys. Rev. Lett.* 68 (7), 1077-1080

- McNamara, G., Alder, B. (1993). "Analysis of lattice Boltzmann treatment of hydrodynamics", *Physica A*, 194, 218-228.
- Alexander, F. J. Chen S., Grunau, D. W. (1993) "Lattice Boltzmann thermohydrodynamics" *Phys. Rev. B* 48, 634.
- Chen, Y., Ohash, H., Akyama, M. (1994). "Thermal lattice Bhatnagar-Gross-Krook model without nonlinear deviation in macrodynamic equations", *Phys. Rev. E*, 50, 2776-2783.
- He, X., Luo, L.S. (1997), "A priori derivation of the lattice Boltzmann equation", *Phys. Rev. E* 55, 6333.

Boundary conditions

- Ginzbourg, I., Adler, P.M. (1994) "Boundary flow condition analysis for the three-dimensional lattice-Boltzmann model" *Journal de Physique II*, 4, 191-214.
- Genabeek, O., Rothman D. (1999). "Critical behavior in flow through a rough-walled channel". *Phys. Letters A*, 255, 31-36.

Multibits and integers models

- Boghosian, B.M., Yenez, J., Alexander, F.J., Margolus, N.H. (1997), " Integer lattice gases", *Phys Rev E* 55(4) 4137-4147

Flow through porous media

- Chen, S., Diemer, K., Doolen, D., Eggert, K., Gutman, S., Travis, B.J. (1991.b). "Lattice gas automata for flow through porous media" *Physica D* 47(1-2), 72-84.
- Kohring, G.A. (1991a). "Effect of finite grain-size on the simulation of flow through porous-media" *Journal de Physique II* 1 (2), 87-90.
- Kohring, G.A. (1991b). "Calculation of permeability of porous-media using hydrodynamic cellular automata" *J. Stat. Phys.* 63 (1-2), 411-418.
- Kohring, G.A. (1992). "The cellular automata approach to simulating fluid-flows in porous media" *Physica A* 186 (1-2), 97-108.
- Gao, Y., Sharma, M.M. (1994). "A LGA model for fluid-flow in heterogeneous porous-media." *Transp. Porous Media* 17 (1), 1-17.
- McCarthy, J.F. (1994). "Flow through arrays of cylinders: lattice-gas cellular automata calculations" *Phys. Fluids* 6(2), 435-437.
- Liang, Z. R., Fernandes, C. P., Magnani, F.S. and Philippi, P. C., (1998) "A Reconstruction Technique of 3-D Porous Media by using Image Analysis and Using Fourier Transform", *Journal of Petroleum Science and Engineering*, 21, 3-4, 273-283
- Santos, L. O. E., P. C. Philippi, M. C. Damiani, and C. P. Fernandes. 2002 (a). "Using three-dimensional reconstructed microstructures for predicting intrinsic permeability of reservoir- rocks based on a boolean lattice gas method". In *Journal Of Petroleum Science And Engineering*, 35 (1-2), 109-124.
- Santos, L. O. E., P. C. Philippi, and M. C. Damiani. 2000 (a). "A Boolean Lattice Gas Method for Predicting Intrinsic Permeability of Porous Media". In *Proceedings of Produccion 2000 / Aplicaciones de la ciencia en la ingeniería de petróleo*, Produccion 2000 / *Aplicaciones de la ciencia en la ingeniería de petróleo*, Foz de Iguazu, 2000.
- Santos, L. O. E., P. C. Philippi, and M. C. Damiani. 2000 (b). "Lattice Gas Methods for Predicting Intrinsic Permeability Of Porous Media". In *Anais do ENCIT 2000, ENCIT 2000*, Porto Alegre, in CD_ROM, ABCM.

Singh, M., Mohanty K.K. (2000). "Permeability of spatially correlated porous media" *Chem. Eng. Sci.* **55**, 5393-5403.

Boolean models for immiscible fluids

- Rothmann, D. H., Keller, J. M. (1988). "Immiscible Cellular-Automaton Fluids" *J. Stat. Phys.* **52**, 1119-1127.
- Chen, S., Doolen G. D., Eggert, K., Grunau, D. and Loh, E. Y. (1991.a). "Local lattice-gas model for immiscible fluids" *Physical Review A* **43**, 7053-7056.
- Santos, L. O. E. 2000. "Desenvolvimento de Modelos de Gás em Rede para Escoamentos Monofásicos e Bifásicos". *Doctoral Thesis*, Mechanical Engineering Department, Federal University of Santa Catarina, 159 p.
- Santos, L. O. E., and P. C. Philippi. 2002 (a), "Lattice-gas model based on field mediators for immiscible fluids", *Physical Review E*, **65** (4), 46305-46312.
- Santos, L. O. E., P. C. Philippi, S. L. Bertoli, and P. C. Facin. 2002 (b), "Lattice-gas Models for Single and Two-Phase Flows: Application to the Up-Scaling Problem in Porous Microstructures" (in press). In *Computational and Applied Mathematics*.
- Philippi, P. C., L. O. E. Santos, S. L. Bertoli, F. Wolf, and P. C. Facin. 2001. "Lattice-gas models for fluid flow" (Invited Lecture). *Brazilian Congress on Mechanical Sciences*, Uberlândia, 2001, 20, 96-116.
- Wolf, F., L. O. E. Santos, and P. C. Philippi. 2002. "Spreading of a liquid drop on a solid surface". In *Computational Modeling of Multi-Scale Phenomena*, Second Symposium on Computational Modeling of Multi-Scale Phenomena, Petrópolis.
- Wolf, F. 2002. "Simulação de processos de deslocamento imiscível utilizando modelos de gás em rede com mediadores de campo". *MSc Dissertation*, Mechanical Engineering Department, Federal University of Santa Catarina

Boltzmann models for immiscible fluids

- Gunstensen, A.K., Rothman D.H., Zaleski S., Zanetti G. (1991) "Lattice Boltzmann Model of Immiscible Fluids", *Physical Review A*, **43** (8), 4320-4327.
- Shan XW, Chen HD (1994) "Simulation of nonideal gases and liquid-gas phase-transitions by the lattice Boltzmann-equation", *Phys Rev E*, **49** (4): 2941-2948.
- Martys NS, Chen HD, (1996), "Simulation of multicomponent fluids in complex three-dimensional geometries by the lattice Boltzmann method, *Phys Rev E* **53** (1), 743-750.
- Facin, P. (2002), "Chapman-Enskog analysis of Boltzmann models for miscible and immiscible fluids", *Doctoral Thesis* (in course), Mechanical Engineering Department, Federal University of Santa Catarina.
- Santos, L. O. E., and P. C. Philippi. 2002 (b). "Prediction of relative permeability in immiscible displacement". In *Computational Modeling of Multi-Scale Phenomena*, Second Symposium on Computational Modeling of Multi-Scale Phenomena, Petrópolis, RJ.
- Facin, P. C., L. O. E. Santos, and P. C. Philippi. 2002. "A new lattice-Boltzmann mesoscale Model for miscible Fluids: Chapman-Enskog asymptotic analysis". In *Computational Modeling of Multi-Scale Phenomena*, Second Symposium on Computational Modeling of Multi-Scale Phenomena, Petrópolis, RJ.

Vortex shedding

- Meneguini, J. R., Siqueira, C. R., Flatschart, R. B., Saltara, F., Ferrari Jr., J. A., "Numerical Simulation of Flow Interference Between two Circular Cylinders in Tandem", *19th International Conference on Offshore Mechanics and Arctic Engineering*, February 14-17, 2000, New Orleans, LA, USA.
- R. Surmas, L. A. Hegele Jr, A. Silveira Neto, P.C. Philippi, L.O. E. dos Santos, 2002. Vortex Shedding from Two-Dimensional Obstacles. In *Computational Modeling of Multi-Scale Phenomena*, Second Symposium on Computational Modeling of Multi-Scale Phenomena, Petrópolis.
- A. L. F. Lima e Silva , R. Surmas, L.O. Emerich dos Santos, P. C. Philippi, A. Silveira Neto, "Comparative numerical simulation of two-dimensional flows over a pair of circular cylinders, disposed in tandem, using immersed boundary and lattice-boltzmann methods", Submitted to: *Conference on Bluff Body Wakes and Vortex-Induced Vibrations BBVIV3*, 17-20 December 2002, Port Douglas Australia.

